

UNCLASSIFIED

AD NUMBER

ADC008887

CLASSIFICATION CHANGES

TO: unclassified

FROM: secret

LIMITATION CHANGES

TO:

Approved for public release, distribution unlimited

FROM:

Distribution limited to U.S. Gov't. agencies only; Test and Evaluation; Dec 76. Other requests for this document must be referred to Director, Naval Research Lab., Washington, D. C. 20375.

AUTHORITY

31 Dec 1991 per document markings; NRL ltr., Ser 1221.1/0005, 2 Feb 1998

THIS PAGE IS UNCLASSIFIED

**SECRET**

NRL Report 8061  
Copy No. 16

ADC008887

# Far Ultraviolet Studies of Missile Trails

[Unclassified Title]

G. T. HICKS, T. A. CHUBB, AND R. R. MEIER

*E. O. Hulburt Center for Space Research*

December 14, 1976

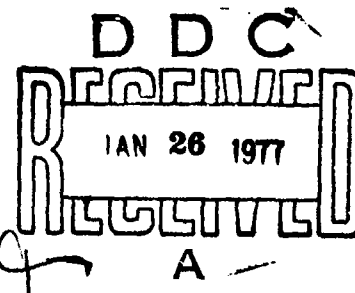
DDC FILE COPY



\*NATIONAL SECURITY INFORMATION\*

"Unauthorized Disclosure Subject to Criminal  
Sanctions"

NAVAL RESEARCH LABORATORY  
Washington, D.C.



SECRET: classified by CONRL.  
Exempt from GDS of E.O. 11652.  
Ex. Cat. (3). Auto. declass. Dec. 31, 1991.

Distribution limited to U.S. Government Agencies only; test and evaluation; December 1976. Other requests for this document  
must be referred to the Commanding Officer, Naval Research Laboratory, Washington, D.C. 20375.

**SECRET**



**SECRET**

**NATIONAL SECURITY INFORMATION**

**Unauthorized Disclosure Subject to Criminal Sanctions.**

**SECRET**

UNCLASSIFIED

SECRET

SECURITY CLASSIFICATION OF THIS PAGE (When Data Entered)

REPORT DOCUMENTATION PAGE		READ INSTRUCTIONS BEFORE COMPLETING FORM
1. REPORT NUMBER NRL Report 8061	2. GOVT ACCESSION NO.	3. RECIPIENT'S CATALOG NUMBER
4. TITLE (and Subtitle) FAR-ULTRAVIOLET STUDIES OF MISSILE TRAILS {Unclassified Title}	5. TYPE OF REPORT & PERIOD COVERED NRL Research Problem	
6. PERFORMING ORG. REPORT NUMBER		7. AUTHOR(s) G. T. Hicks, T. A. Chubb, and R. R. Meier
8. CONTRACT OR GRANT NUMBER(s) Program Element 61153N-34		9. PERFORMING ORGANIZATION NAME AND ADDRESS Naval Research Laboratory Washington, D.C. 20375
10. PROGRAM ELEMENT, PROJECT, TASK AREA & WORK UNIT NUMBERS Program Element 61153N-34 RR 034-06-42, 71A01-61		11. CONTROLLING OFFICE NAME AND ADDRESS Office of Naval Research Arlington, Va. 22217
12. REPORT DATE December 14, 1976		13. NUMBER OF PAGES 37
14. MONITORING AGENCY NAME & ADDRESS (if different from Controlling Office)		15. SECURITY CLASS. (of this report) SECRET 15a. DECLASSIFICATION/DOWNGRADING SCHEDULE X6DS-3 (1991)
16. DISTRIBUTION STATEMENT (of this Report) Distribution limited to U.S. Government Agencies only; test and evaluation; December 1976. Other requests for this document must be referred to the Commanding Officer, Naval Research Laboratory, Washington, D.C. 20375.		
17. DISTRIBUTION STATEMENT (of the abstract entered in Block 20, if different from Report)		
18. SUPPLEMENTARY NOTES		
19. KEY WORDS (Continue on reverse side if necessary and identify by block number) Attack assessment      Surveillance Early warning      Tactical intelligence FUV      VUV Midcourse vectoring Missile warning		
20. ABSTRACT (Continue on reverse side if necessary and identify by block number) (U) Far-ultraviolet studies of missile trails have been conducted within the Navy Astronomy and Astrophysics Subelement. Observational and analytical studies of the Hicks effect have been conducted; surveillance aspects of this effect have been examined.		

DD FORM 1473  
1 JAN 73EDITION OF 1 NOV 65 IS OBSOLETE  
S/N 0102-014-6601

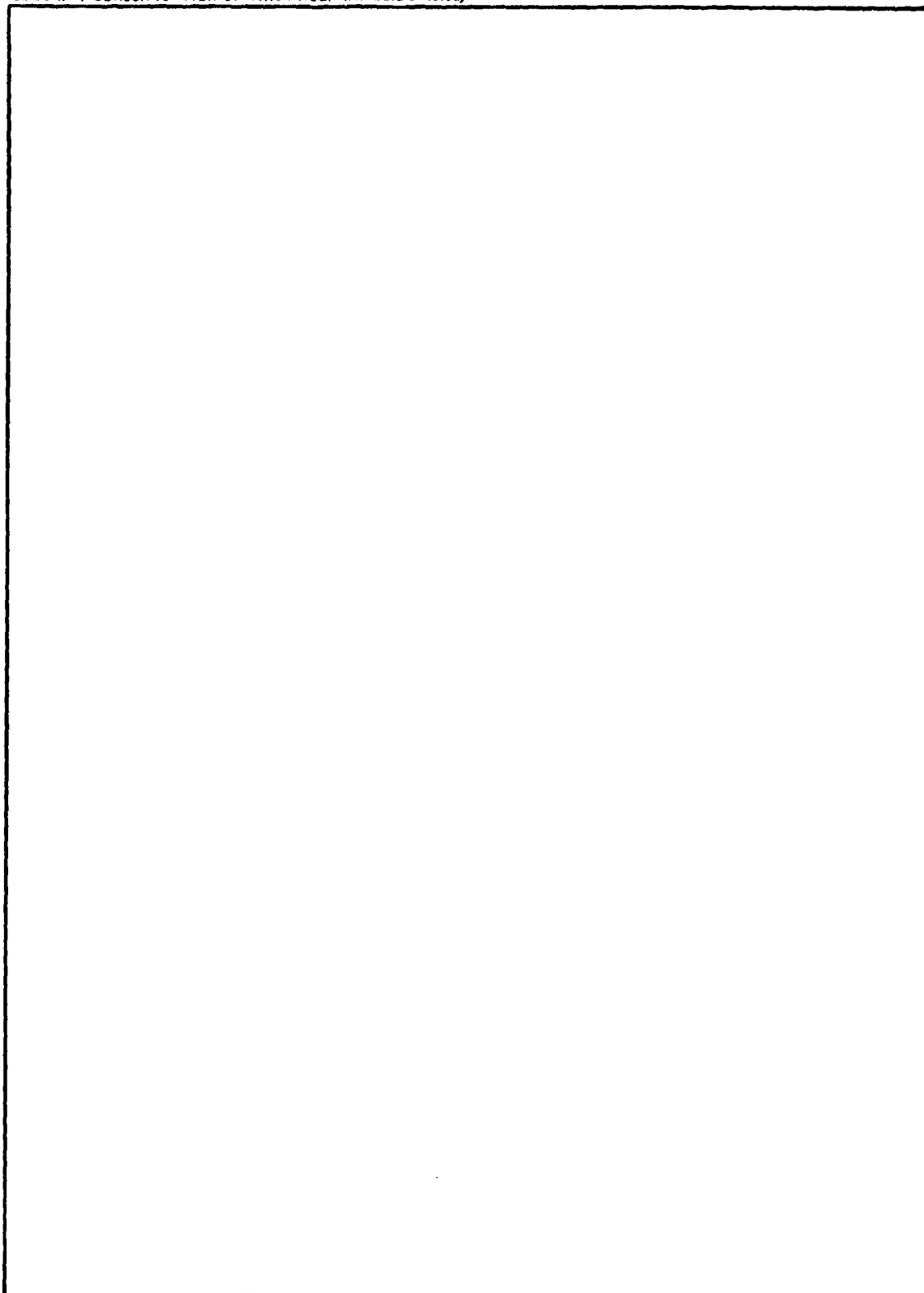
UNCLASSIFIED

SECRET

(This page is unclassified)

**UNCLASSIFIED**

SECURITY CLASSIFICATION OF THIS PAGE(When Data Entered)



ii

**UNCLASSIFIED**

SECURITY CLASSIFICATION OF THIS PAGE(When Data Entered)

**SECRET**

## CONTENTS

INTRODUCTION .....	1
FAR-ULTRAVIOLET OBSERVATIONS FROM SPACE .....	2
HICKS EFFECT OBSERVATIONS .....	5
APOLLO 6 OUTGASSING AND FUEL DUMPS .....	8
INTERPRETATION OF OGO 4 OBSERVATIONS .....	11
SUMMARY, CONCLUSIONS, AND RECOMMENDATIONS ...	13
REFERENCES .....	14
APPENDIX A — Far-Ultraviolet Observations of Earth From the Moon .....	17
APPENDIX B — Summary of Hicks Effect Events .....	23
APPENDIX C — Calculations Concerning Detection of High- Altitude Missile Burns (Above 150 km) Using Hicks Effect .....	25
APPENDIX D — Observability of Hicks Effect at 120 km .....	31
APPENDIX E — Detection of Missiles by Line-Wing Radiation Below 100 km .....	33

1. ☐ 2. ☐ 3. ☐ 4. ☐ 5. ☐ 6. ☐ 7. ☐ 8. ☐ 9. ☐ 10. ☐ 11. ☐ 12. ☐ 13. ☐ 14. ☐ 15. ☐ 16. ☐ 17. ☐ 18. ☐ 19. ☐ 20. ☐ 21. ☐ 22. ☐ 23. ☐ 24. ☐ 25. ☐ 26. ☐ 27. ☐ 28. ☐ 29. ☐ 30. ☐ 31. ☐ 32. ☐ 33. ☐ 34. ☐ 35. ☐ 36. ☐ 37. ☐ 38. ☐ 39. ☐ 40. ☐ 41. ☐ 42. ☐ 43. ☐ 44. ☐ 45. ☐ 46. ☐ 47. ☐ 48. ☐ 49. ☐ 50. ☐ 51. ☐ 52. ☐ 53. ☐ 54. ☐ 55. ☐ 56. ☐ 57. ☐ 58. ☐ 59. ☐ 60. ☐ 61. ☐ 62. ☐ 63. ☐ 64. ☐ 65. ☐ 66. ☐ 67. ☐ 68. ☐ 69. ☐ 70. ☐ 71. ☐ 72. ☐ 73. ☐ 74. ☐ 75. ☐ 76. ☐ 77. ☐ 78. ☐ 79. ☐ 80. ☐ 81. ☐ 82. ☐ 83. ☐ 84. ☐ 85. ☐ 86. ☐ 87. ☐ 88. ☐ 89. ☐ 90. ☐ 91. ☐ 92. ☐ 93. ☐ 94. ☐ 95. ☐ 96. ☐ 97. ☐ 98. ☐ 99. ☐ 100. ☐

**SECRET**

**SECRET**

**OBSERVATIONS OF HYDROGEN LYMAN ALPHA EMISSION  
FROM MISSILE TRAILS**  
[Secret Title]

**Abstract:** (S) Through the NRL far-ultraviolet experiment on the OGO 4 satellite, it was accidentally discovered that during the passage of missiles through the upper atmosphere of Earth hydrogenous exhaust products are deposited along their trajectories. This deposition results in a local enhancement of hydrogen, which resonantly scatters Lyman  $\alpha$  ( $\text{Ly } \alpha$ ) radiation from the Sun and from the atmosphere (the Hicks effect). The local enhancement of radiation has been observed to be as much as 37% above the natural background. As a result of the minute quantities of atomic hydrogen required for enhancement of this glow, the Hicks effect provides the most sensitive means of observing high-altitude missiles yet discovered, permitting observation of small high-altitude burns under both sunlit and night conditions.

(S) The purpose of this report is to present a summary of the OGO 4 observations and to assess the military potential of the phenomenon with respect to surveillance and intelligence. In this regard, it is important to note that calculations indicate that signatures of the Hicks effect include both a prompt localized emission suitable for early warning, tracking, and attack assessment, followed by development of an extended diffuse cloud suitable for tactical intelligence investigations.

**INTRODUCTION**

(S) In July 1967 an experiment provided by the Naval Research Laboratory was launched into orbit on the NASA Orbiting Geophysical Observatory (OGO 4). The purpose of the experiment was to provide baseline information about the far-ultraviolet (FUV) radiation field of the upper atmosphere of the Earth. Far-ultraviolet radiation (1000 to 2000 Å) is also referred to as "vacuum ultraviolet" (VUV), and sometimes as "extreme ultraviolet" (EUV). During the routine analysis of data from that experiment, an anomalous signal was observed in one of the photometric channels. Subsequently, this event was shown to be associated with the launch of an Atlas missile. The signal was attributed to resonant scattering of sunlight by atomic hydrogen produced along the trajectory of the missile. The observability of missiles in the light of hydrogen (the Lyman  $\alpha$  emission line) was termed the "Hicks effect" by T. A. Chubb [1], because G. T. Hicks discovered this phenomenon. This discovery was first reported in an unpublished NRL report\* in 1971 and again by Chubb at the 1973 FUV Plume Meeting at the Institute for Defense Analysis (IDA) [1].

(S) Since the discovery of the Hicks effect, 23 events have been found in the OGO 4 data. All but one of the events occurred during the day. All have been identified with specific missile launches.

\*The following initial report received limited circulation: G.T. Hicks, T.A. Chubb, R.R. Meier, and R.J. Veith, "Observations of Atmospheric Scars Produced by High Altitude Missiles," unpublished report, Naval Research Laboratory, Washington, D.C. (Secret Report, Unclassified Title), May 1971.

Manuscript submitted September 1, 1976.

**SECRET**

(S) The purpose of this report is to provide a final report of the OGO 4 observations. We begin by discussing the natural FUV environment, against which the perturbing influences of the missile passage must be seen. Next, we describe the discovery of the Hicks effect and show various examples of the phenomenon. Then we present a quantitative interpretation of the results. Finally, we provide an assessment of the current knowledge concerning the Hicks effect and its potential for contribution to such areas of Department of Defense (DOD) interest as tactical intelligence, early warning, and attack assessment.

## FAR-ULTRAVIOLET OBSERVATIONS FROM SPACE

(U) In this section we discuss the OGO 4 experiment and its observations of the naturally occurring FUV Earth environment. Additional studies of the FUV radiation field of the Earth were provided by the NRL experiment of G. R. Carruthers [2] flown on the Apollo 16 mission. Photographic FUV observations of Earth obtained by Carruthers are discussed in Appendix A, as a supplement to this section.

(S) The OGO 4 Satellite was launched July 28, 1967. It was a controlled-orientation satellite in a polar orbit, and it always maintained the same side facing Earth. Its altitude ranged from 925 km (575 mi) to 418 km (260 mi). Naval Research Laboratory equipped OGO 4 with a set of Earth-facing FUV radiometers for studying airglow and auroras. Characteristics of the instrument are given in Table 1, taken from the paper by Chubb and Hicks [3]. The data were displayed as a series of graphs showing the glow intensity beneath the satellite, and global maps were obtained as the Earth rotated inside the satellite orbit. Because of orbital precession, data were obtained at all Sun orbits; intensity plots were obtained for midnight-midday orbits, dawn-dusk orbits, and orbits in between. In Fig. 1 we show data from a midnight-midday orbit. It is important to understand this orbital record of airglow intensity, because the Hicks effect shows up as a perturbation of the natural scene. We will, therefore, examine this plot of the natural background in detail before considering the discovery of the Hicks effect.

(U) The record shown in Fig. 1 starts off with the OGO 4 satellite over the Equator on the dark side of the Earth. The satellite is moving north. The top graph shown is the response of a radiometer sensitive almost exclusively to light produced by  $N_2$  molecules (1425 to 1500 Å). A radiometer sensitive to atomic oxygen emissions would have recorded a similar scene. The radiometer viewed a wide patch of air below the satellite. The airglow originates at an altitude of about 110 km (70 mi), and at this altitude the radiometer views a circle averaging about 560 km (350 mi) in diameter. At night over the Equator, the nitrogen radiometer sees no glow. This situation continues until the satellite enters the region of the aurora borealis (0544 GMT). The radiometer then records two brightly glowing auroral display regions before crossing over the interior of the auroral oval.

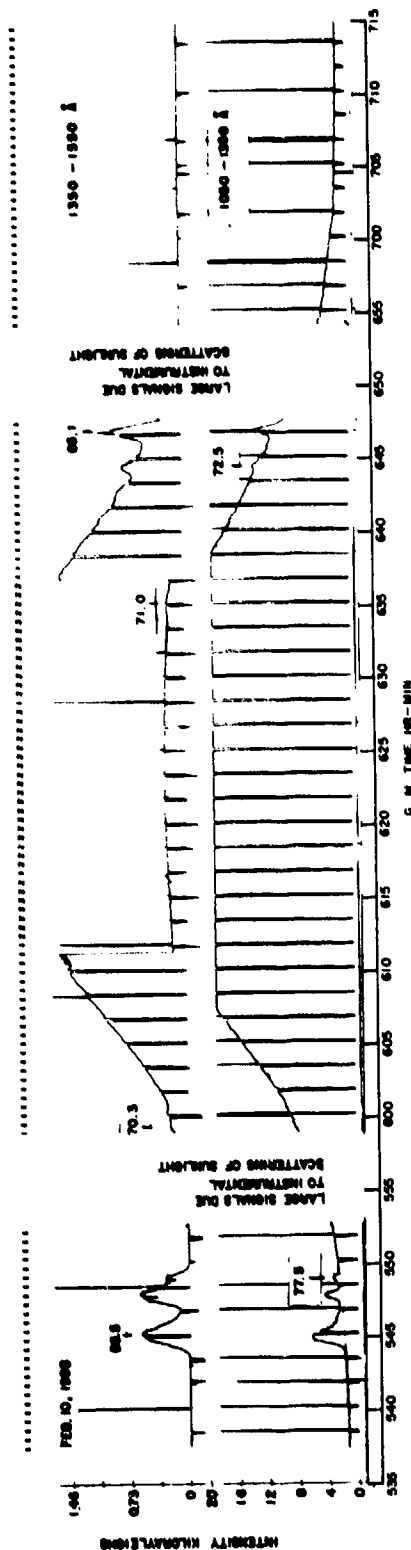
(U) As the satellite enters sunlight, data are missing because of an instrumental light-scattering problem. As the satellite moves into the dayside of the Earth, the data again become valid. We see now at 0624 a peaking of the main glow region of the Earth, the day airglow. (An automatic scale change for the instrument occurs at 0611.5, decreasing the plotted amplitude between 0611.5 and 0637.) As the satellite moves toward the dark side of the Earth, auroras are observed over Antarctica. These auroras



(U) Table 1 — Far-Ultraviolet Sensors in OGO 4

Chamber Range (Å)	Direction	Type of Chamber <sup>a</sup>	Window		Filling		Direction of View <sup>†</sup>	Sensitive Area (cm <sup>2</sup> )	Geometric Factor (cm <sup>2</sup> sr)	Extreme Full Angle of View (deg, min)		Preflight Quantum Yield at Reference Angle	Probable Source of Response	Emission Wavelength (Å)	System Calibration (LE/V)
			Material	Thickness (mm)	Gas	(X 100 Pa)	Pressure (mm of Hg)								
1050-1350	Up	Single ion	LiF	2	NO	27 ± 7	20 ± 5	15°	0.70	0.019	21° 40'	0.48	H	1216	7.61
1050-1350	Down	Single ion	LiF	2	NO	27 ± 7	20 ± 5	CE	0.70	0.041	32° 10'	0.40	H, O, N	1216 1216 1304 1200	4.27
1230-1350	Down	Set 3	CaF <sub>2</sub>	2	NO	27	20	CE	2.10	1.13	65° 40'	0.25	O <sup>‡</sup>	1304	0.23
1350-1550	Down	Set 3	BaF <sub>2</sub>	1	UDMH <sup>§</sup>	7	5	CE	2.10	1.13	65° 40'	0.13	N <sub>2</sub> <sup>§</sup>	1375-1500	0.36

<sup>a</sup>Single ion = single ion chamber; set 3 = set of 3 ion chambers.<sup>†</sup>15° = 15° away from zenith in direction away from Sun. CE = toward center of Earth.<sup>‡</sup>Almost all.<sup>§</sup>UDMH = unsymmetrical dimethylhydrazine.<sup>¶</sup>Predominantly.



(U) Fig. 1 — Intensity vs time of far ultraviolet airglow and aurora, as recorded by two downward-looking photometers aboard OGO 4. One orbit of data is shown. The orbit is for a time when the Sun lies close to the orbited plane. Hence, most of the data are for near-midnight and near-midday conditions. Before 0553 and after 0654, both satellite and substellite points are in the night. Auroras are observed 0544 to 0550, 0559.5, 0635, and 0642-0648. All these auroras are sunlit except those seen 0544-0550. The invariant latitudes at which the arcs were crossed are shown by block numbers above the auroral signals. Between about 0603 and about 0641, the responses of both photometers are dominated by day airglow signals. Between 0611.3 and 0636.8, the 1350- to 1550-Å photometer is operating in a reduced sensitivity mode. Between 0550 and 0553, the satellite is inside the auroral oval, and the 1350- to 1550-Å sensor records a black sky like that seen at night equatorward of the auroral display. Every 100 s there is a zero check of the instrument, causing a downward excursion in the signal. Occasionally these are accompanied by a noise spike.

would not be seen by a viewer on the surface of the Earth because of overhead daylight, but they show up clearly looking down from space in the FUV because of the enormously reduced intensity of daylight in the FUV. In the FUV, the Earth is really quite dark; the strongest signal shown by the nitrogen radiometer corresponds to an airglow intensity of  $2.5 \times 10^{-10} \text{ W}\cdot\text{cm}^{-2}\cdot\text{sr}^{-1}$  integrated over the whole 1375- to 1500-Å band. This compares with an infrared (IR) emission of about  $8 \times 10^{-6} \text{ W}\cdot\text{cm}^{-2}\cdot\text{sr}^{-1}$  in a 1-μm band at 3 μm.

(S) The second graph in Fig. 1 shows a record of the airglow as seen largely in hydrogen light. The hydrogen radiometer was collimated more tightly than the nitrogen radiometer, but still viewed a circle of 185-km (115 mi) average diameter at the 113-km (70 mi) glow altitude. The hydrogen radiometer sees much the same scene as the nitrogen radiometer, except that the hydrogen radiometer records glowing hydrogen beneath the spacecraft even at darkest midnight. Also, the hydrogen radiometer shows differences in the hydrogen brightness of the two auroral arcs observed by the nitrogen radiometer. The first arc at 0545 has a relatively strong emission in hydrogen light and is a proton aurora. In no cases have we observed an aurora showing a significantly higher ratio of hydrogen light to nitrogen light than that shown at 0545. This point is emphasized because the Hicks effect shows up as a local increase in hydrogen glow with no increase in nitrogen or oxygen emissions.

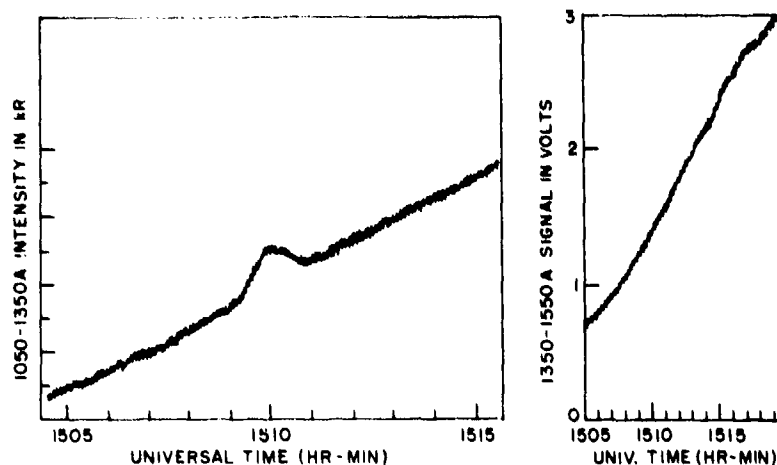
(S) Airglow and aurora records of the type shown in Fig. 1 were obtained for a major portion of the 17 months of OGO 4 life. Time and spatial variations of the aurora were studied and are reported in Chubb and Hicks [2]. Extensive studies of the natural airglow were made by Meier and his colleagues; e.g., Meier and Mange [4]. Equatorial oxygen FUV emissions were discovered by Hicks and Chubb [5]. All in all, an extensive quantity of data has been examined. Based on these studies, a good understanding of the behavior of the natural background is in hand. The signatures of the Hicks effect, which we will next discuss, were easily distinguished from all naturally occurring events. It is with this experience that we can confidently state that no natural phenomenon mimics the man-made perturbation produced by a high-altitude rocket firing.

#### (S) HICKS EFFECT OBSERVATIONS

(U) We have seen a typical orbit of data for the OGO 4 experiment in Fig. 1. The main characteristic of these data is a smooth intensity variation with maximum signals seen at noon and minimum signals occurring at midnight. In addition, superimposed upon the smoothly varying signal amplitude is an enhanced signal at various parts of the orbit. These enhanced signals result from the polar aurora and are seen with both photometric channels.

(S) During examination of November 16, 1968 data, for auroral signals during a polar cap absorption (PCA) event, it was noticed that a rather large enhancement of signal occurred in the 1050- to 1350-Å channel with no enhancement whatsoever in the 1350- to 1550-Å channel. (See Fig. 2.) The local time of this observation was about 9:00 a.m. This finding was rather puzzling, and attempts were made to explain what was happening. Because it was known that a PCA event was in progress and that such an event is caused by large numbers of high-energy protons precipitating over a wide area of the polar region, creating an increase in hydrogen emissions throughout the spectrum, the possibility was considered that a pure hydrogen-arc emission of Ly α was responsible for the results seen

ATLAS 56F (KX-110)  
16 NOVEMBER 1968 1201 6 UT



(S) Fig. 2 — Hicks effect signal from Atlas 56F (KX-110). Notice the absence of any enhancement in the longer wavelength channel plotted on the right (with a smaller time scale). Details of the event are given in Appendix B.

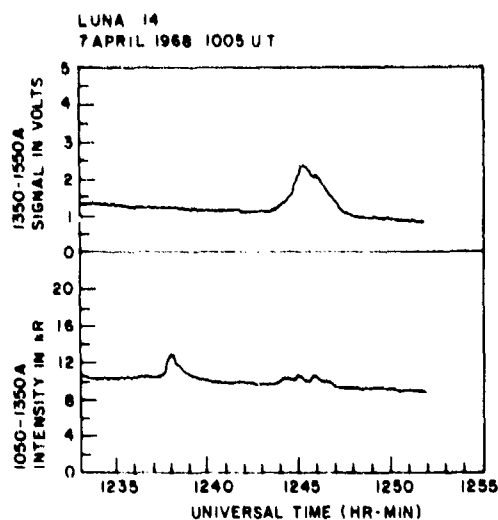
in Fig. 2. However, when the geographic position of the event was determined to be off the coast of California, very localized, and occurring at no other place in that particular orbital pass, we concluded that the event did not result from a PCA.

(S) The possibility that another satellite had passed under OGO 4 at this particular time was considered. A search was made of all data pertaining to space objects at lower altitudes that might have been in the field of view of our detectors at this time, with negative results. A similar search was made of meteors and meteorites, again with negative results. Next, a search was made of the data pertaining to missile launches from Vandenberg before the event mentioned. This search was successful. It was learned that an Atlas KX-110 had a trajectory that passed close to the point in question. Recognizing that this finding seemed the most promising explanation of our observations, we began to search our OGO 4 data for similar signatures and to check such events against times of passage over known missile burn areas. This effort resulted in our finding 23 cases of strong confirmation of Soviet and U.S. missile launches with positive observations obtained at times ranging from about 6 min to 10 h after launch. Figures 3 and 4 display additional examples of the Hicks effect to illustrate the purity of the hydrogen signal compared to that of the longer wavelength channel for such events. Figure 5 shows the only nighttime event seen by the OGO 4 experiment. Only data from the Ly  $\alpha$  channel are displayed in Fig. 5 because the other channel gave no signal. The spacecraft was over the U.S.S.R. at the time of the observation.

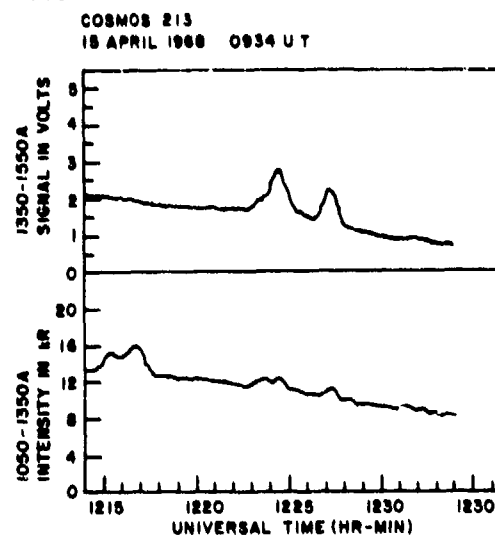
(S) Figure 6 shows observation made during the Apollo 6 mission, when large quantities of H<sub>2</sub> were dumped.

SECRET

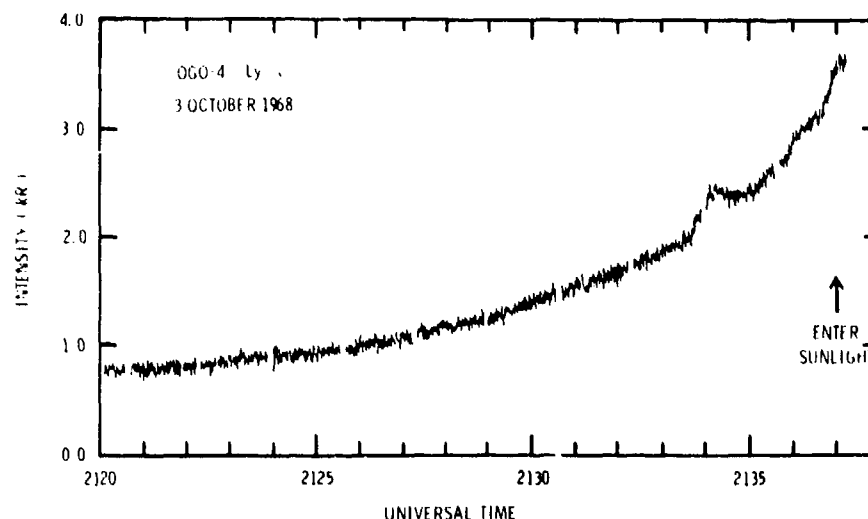
NRL REPORT 8061



(S) Fig. 3 — Hicks effect signal from Luna 14. The event can be seen near 1238 UT in the Ly  $\alpha$  channel (1050 to 1350 Å). Auroras are seen in both channels near 1246 UT. On the scale of this figure, naturally occurring perturbations of the background always display a larger signal in the 1350- to 1550-Å channel than in 1050- to 1350-Å one. Details of the event are given in Appendix B.



(S) Fig. 4 — Hicks effect signal from Cosmos 213. The event near 1215 UT can be compared to aurora signals at 1224 and 1227 UT. Details of the event are given in Appendix B.



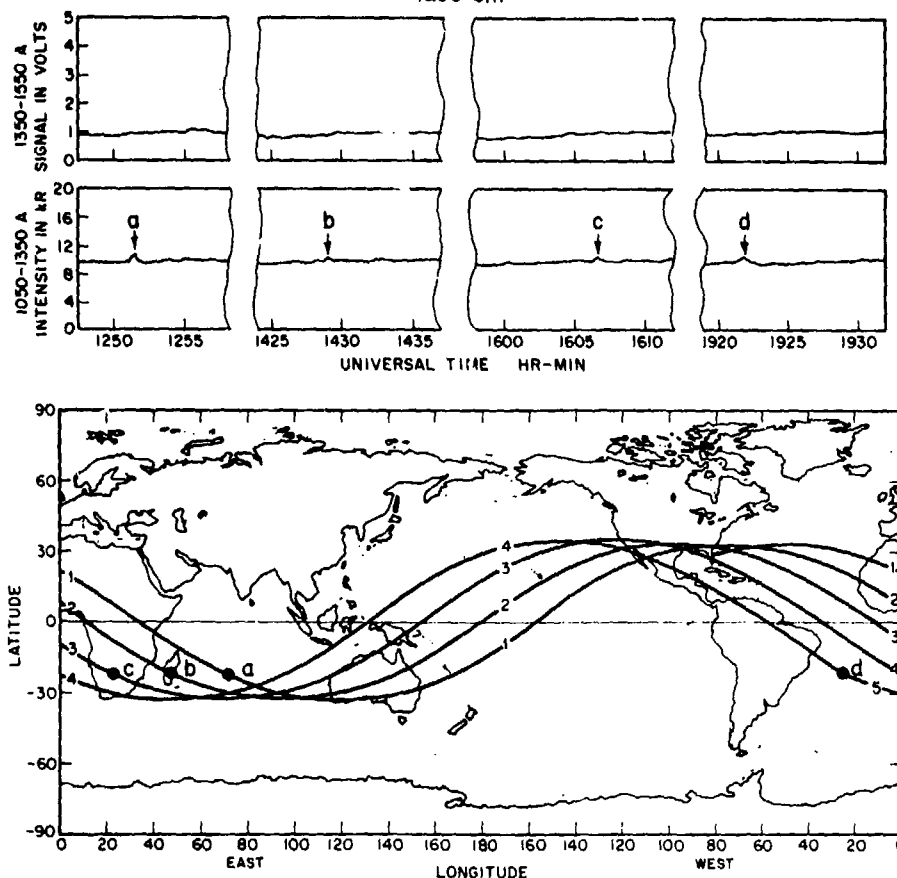
(S) Fig. 5 — Nighttime Hicks effect in 1050- to 1350-Å channel. The perturbation is seen at 2134 UT. No signal was seen in the 1350- to 1550-Å channel. The Sun-Earth-satellite angle was  $124^\circ$  and the spacecraft was inside the shadow of the Earth until 2137 UT. Details of the event are given in Appendix B.

SECRET

## APOLLO 6 MISSION

4 APRIL 1968

1200 U.T.



(a)

(S) Fig. 6 — Observation of the Apollo 6 mission. Details of the events are described in the test and in Appendix B.

(S) A tabular listing of the 23 events obtained by the OGO 4 experiment is given in Appendix B, along with pertinent information relating to the observation conditions and the associated launches.

(S) The characteristics of the OGO 4 observations led us to suggest that the emission resulted from the Ly  $\alpha$  emission line of atomic hydrogen, which might be associated with exhaust products in the missile trail [1]. The discussion in a later section demonstrates the plausibility of this interpretation.

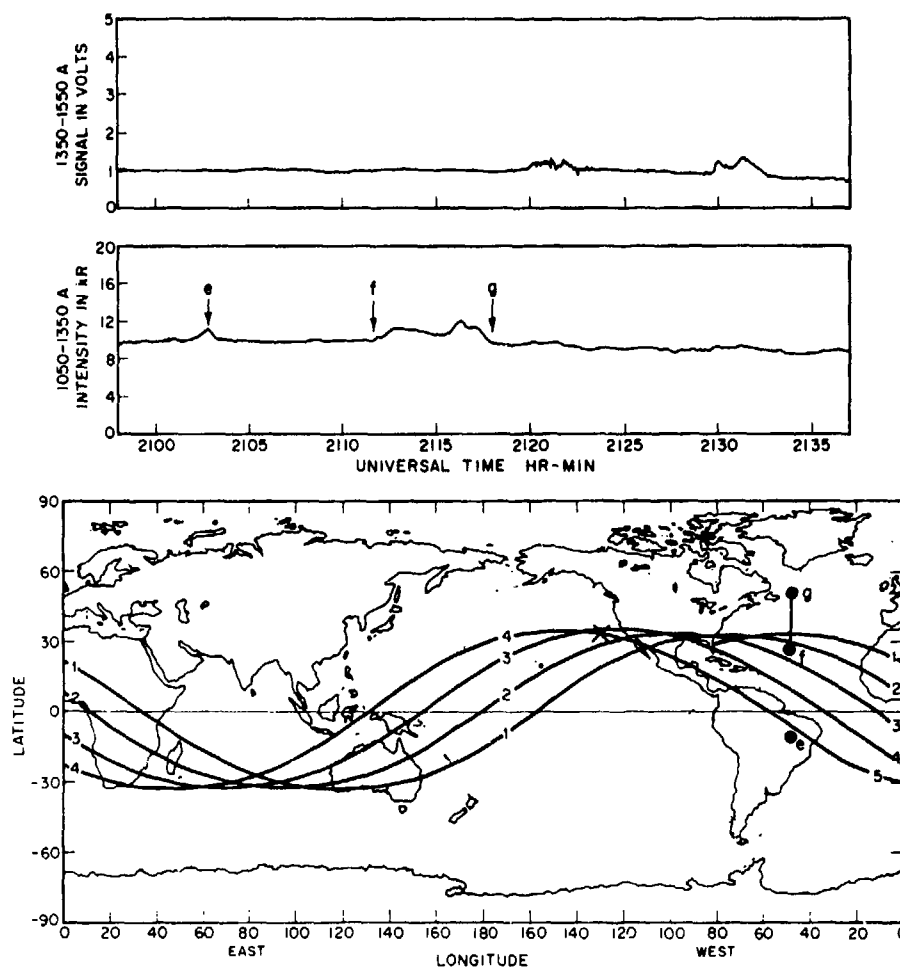
#### (S) APOLLO 6 OUTGASSING AND FUEL DUMPS

(S) Observations by the OGO 4 experiment of the Apollo 6 mission were of special interest because there were malfunctions in restarting the SIVB engine and a very large

SECRET

NRL REPORT 8061

APOLLO 6 MISSION (CONT'D)

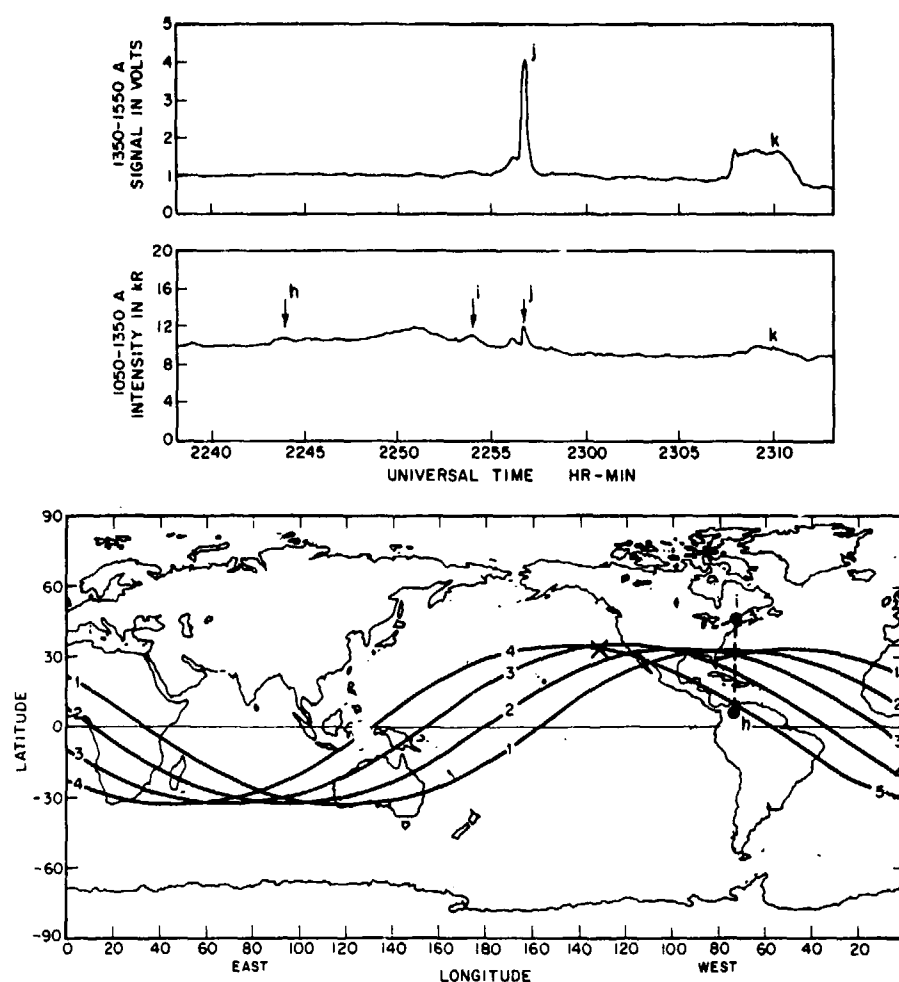


(b)

(S) Fig. 6 — Observation of the Apollo 6 mission. Details of the events are described in the test and in Appendix B.

amount of fuel was left on board. The fuel was subsequently vented later in the mission. Apollo 6 was launched on April 4, 1968, at 1200.00 UT. The initial burn of the SIVB was cut off at 1212.45 UT at latitude  $32.74^{\circ}\text{N}$ ,  $50.16^{\circ}\text{W}$  at an altitude of 190.8 km (130.0 n.mi.) traveling at orbital velocity. At 1251.4 the OGO 4 satellite was at  $23.5^{\circ}\text{S}$ ,  $72.4^{\circ}\text{E}$  at an altitude of 443.7 km (239.6 n.mi.) when the signal marked "a" in Fig. 6a was recorded. A rough calculation shows that the Apollo 6 was at this latitude and longitude at approximately 1245 UT or 6 min prior to the passage of OGO 4. Neither engine of the Apollo 6 was burning at 1245, but the SIVB was leaking fuel on the first three orbits, as we subsequently learned. We attribute the weak signals "a," "b," and "c" to this leaking of  $\text{H}_2$ . It should be emphasized that the leaking must have occurred continuously during these orbits (and probably from early in the mission) for OGO 4 to detect these results, regardless of the proximity of the spacecraft orbits.

## APOLLO 6 MISSION (CONCL'D)



(c)

(S) Fig. 6 — Observation of the Apollo 6 mission. Details of the events are described in the test and in Appendix B.

(S) On the fourth orbit of Apollo 6, no signal was seen by OGO 4, which had crossed the Apollo 6 orbit at nearly 1744.3 UT. The SIVB engine (when it could not be restarted) was separated from the command and service module at 1514.47 UT at latitude  $32.16^{\circ}\text{N}$ ,  $85.11^{\circ}\text{W}$  and shortly thereafter the sustainer propulsion engine (SPE) was fired to drive the payload into a high-altitude ballistic orbit. The SIVB continued in Earth orbit with a heavy load of unburned fuel, as mentioned. At 1807.07 UT at  $32.5^{\circ}\text{N}$ ,  $132.4^{\circ}\text{W}$  (marked as X in Fig. 6) venting of hydrogen from the SIVB was begun and no doubt was accomplished rather quickly. The OGO 4 satellite crossed the orbit of the SIVB at the points marked "d," "e," and "h" at the indicated times. The signals seen by OGO 4 were caused by traces of fuel being vented after the deliberate dump at 1807.07 UT. The large signals covering the extensive areas between "f" and "g" and between "h" and "i" are not readily explainable. However, it should be noted that these successive



orbits were the first crossings by OGO 4 of the launch area at Cape Canaveral and the signals could be Hicks effect residuals from the launch. If this interpretation is correct, the exhaust gases would have traveled essentially in a northerly direction about 2800 km (1500 n.mi.) in 9 h or approximately 74 m/s (165 mi/h.)

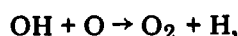
(S) We do not know the rate at which hydrogen fuel was leaking (no doubt inadvertently) on the first three orbits of Apollo 6, nor do we know at what rate the large dump of fuel was made and, from that, the amount of fuel present at "d," "e," and "h." However, it is evident from these observations that very small amounts of fuel vented to the atmosphere create a detectable Ly  $\alpha$  signal during the daytime.

#### (U) INTERPRETATION OF OGO 4 OBSERVATIONS

(S) Following the discovery of the UV "scars," an interpretation of the phenomena involving resonance scattering of sunlight by atomic hydrogen in an optically thick missile trail was presented by Chubb [1]. This interpretation was presented informally to H. G. Wolfhard of IDA, and it is summarized in original form in Appendixes C, D, and E. Since that time, a number of other groups [6-9] have performed similar calculations. Some of these have included estimates of the effects of photochemistry and diffusion. The interested reader can refer to the references mentioned or to Appendixes C to E for details of the calculations. In this section we intend only to give a brief summary of the study of this phenomenon and expected results from these interpretative exercises.

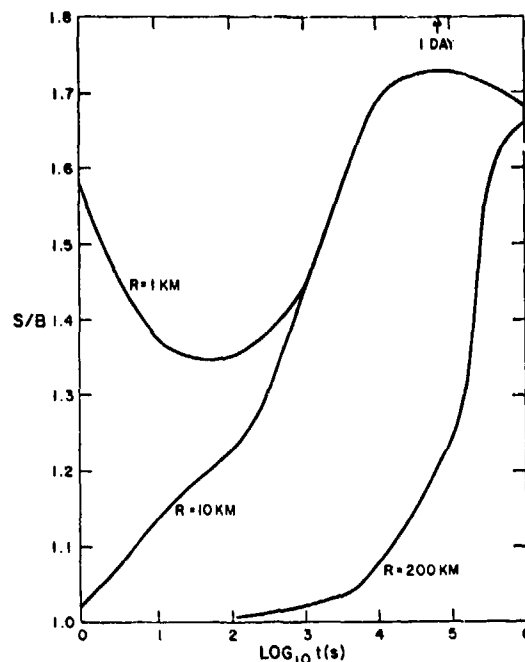
(S) It seems to be clear that a large fraction (approximately 50%) of exhaust products of liquid-fuel rocket engines contain hydrogen. Although the bulk of this hydrogen is in H<sub>2</sub> and H<sub>2</sub>O, frozen equilibrium calculations of rocket nozzle expansions [9] (see also earlier citations of references [5-8]) indicate that atomic hydrogen may be as much as 10% of the H<sub>2</sub>O content. The validity of these calculations is supported by an atomic-hydrogen exhaust observation made during the Mariner 7 mission [11]. Thus, from both theory and experiment, we can safely assume that hydrogen is available in rocket exhaust in both molecular and atomic forms.

(S) The picture that has emerged from the various theoretical efforts [5-8] is that there are two main phases associated with the production of H in missile exhausts. First, atomic hydrogen is produced directly as an exhaust product. The concentrations expected seem to be adequate to give a signature (above the ambient background) immediately during rocket burn as a result of resonant scattering of sunlight. (See Appendixes C to E and Refs. 6 to 9.) This conclusion is of great importance in considering systems applications. The initial glow is relatively short lived (less than 1 h) because the hydrogen atoms rapidly diffuse away. In the meantime, atmospheric reactions with H<sub>2</sub>,



and photodissociation of water by sunlight





(S) Fig. 7 — Estimate of signal-to-background ratio  $S/B$  for  $Ly\alpha$  as a function of time for several field-of-view diameters [7].

begin to provide additional sources of hydrogen atoms on a longer time scale (0.5 h and longer). The importance of these sources at various altitudes is discussed in detail by Ching et al. [5].

(S) From the characteristics of the OGO 4 observations described earlier (observation at times greater than 0.10 h after plume passage and diffusive spreading, one concludes that the OGO 4 scars are the result of the photochemical production of atomic hydrogen. According to diffusion arguments [6], the main source of the radiation glow is probably around 140 km. Although detailed calculations have been performed only for specific cases, such as an Apollo second stage or an Atlas, it seems clear that in general, there is no difficulty in quantitatively accounting for the signal-to-background levels observed by the OGO 4. (See Appendixes C and E and Refs. 5 to 8).

(S) To illustrate this phenomenon, we reproduce in Fig. 7 the example of Myer and Kivel [8], which displays the signal to background expected from an Apollo second stage burn at 120 km. The parameter  $R$  indicates the signal expected from different fields of view. With a high angular resolution instrument such as would be used in operational systems (one that can resolve 1 km or so), the direct (initial) deposition of hydrogen accompanying the burn should be observable. The OGO 4 instrument had poor angular resolution (200 km), so that the airglow background would have obscured most of the initial signal. (Unfortunately, no test of the OGO 4 real-time detection capability occurred.) As can be seen in Fig. 7, when the photochemical phase takes over, the signal rises rapidly. Diffusion acts to spread out the source region and fill the large field of view after  $10^3$  to  $10^5$  s. At 150 km, diffusion would be more rapid, and the wake would

be visible earlier. The signal-to-background ratios observed ( $\leq 1.37$ ) agree well with the predictions of Fig. 7. These results and those of the other groups [6-9] and Appendixes C to E all demonstrate that the physical mechanism of glow enhancement is well understood.

(S) The previous discussion and previous reports [6-9] have considered the possibility of only daytime observations. One nighttime observation has been made (Fig. 5). The energy source at night is indirect solar radiation, radiation multiply scattered into the shadow of the Earth by ambient hydrogen atoms in the atmosphere. (See Figs. 1 and A1.) We have attempted to model the nighttime event. However, the interaction between the diffuse ambient radiation field and the missile trail is very difficult to compute. We have made various approximations by assuming that the source can be represented by a spherically symmetric diffuse mirror. These estimates indicate the plausibility of the interpretation. However, the answers depend strongly on the geometry of the source and its illumination. Thus, no detailed quantitative calculations of nighttime effects have been performed.

#### (U) SUMMARY, CONCLUSIONS, AND RECOMMENDATIONS

(S) As reviewed in the last section, a number of studies have been undertaken to assess our initial suggestion that atomic hydrogen produced in missile trails is responsible for the anomalous signals seen by the OGO 4 instrument. Although the examples chosen in each study (Appendixes C to E and Refs. 5 to 8) vary widely in assumptions and applicability, the common conclusion of all of them is that the interpretation is correct. The interpretative work has indicated that two phases of atomic-hydrogen production take place as the result of the passage of missiles through the upper atmosphere. The first phase is the direct production of atomic hydrogen during engine burn (and possibly outgassing). (Other species such as  $H_2$  or CO will also fluoresce under the action of sunlight.) This direct production of hydrogen is important in relation to prompt detection of missiles as they penetrate the upper atmosphere. Also, midcourse orbital burns may be detectable if sufficient quantities of hydrogen are promptly released. The only experimental evidence for prompt H deposition comes from Mariner hydrazine burns in deep space [11].

(S) The second phase of hydrogen production comes from the interaction of exhaust products with the ambient atmosphere, yielding H, which then resonantly scatters Ly  $\alpha$  radiation. This is the source observed in the bulk of the OGO 4 sightings. Although no opportunity was available to observe prompt emission by OGO 4, the shortest time interval between missile passage and observation was 6 min, and the longest was 10 h.

(S) Even though the physical processes responsible for the Hicks effect signatures now seem to be well understood, there is still a complete lack of real-time, high-angular-resolution observations of rocket plumes. In Appendixes C, D, and E, we have worked out the potential capability of a camera system designed to provide such information both from a low-altitude spacecraft and from synchronous orbit. Included in our calculations are estimates of the signal contrast expected from engine burns of various sizes. To summarize these estimates briefly, a 418-kg (920 lb) engine may produce a 30% contrast at 150 km or above; an 1800-kg (4000 lb) one will yield 7% at 120 km; and a

32 000-kg (70 000 lb) one will yield 3% at 85 to 100 km. Calculations by other groups suggest values that are at least as favorable as these (Fig. 7).

(S) Although the surveillance applicability of these results is obvious, a rather significant intelligence relationship is also indicated. For example, a catalog of hydrogen exhausts from a wide variety of missiles would provide base line data against which new technological developments could be assessed. Also, H<sub>2</sub> and CO emissions along with those of H would be of great use in such a catalog for the same reason.

(S) We believe that the observability of missile trails in the far ultraviolet has significant applicability in the areas of early warning, attack assessment, midcourse maneuvers, and tactical intelligence both during the day and at night. We recommend that the Department of Defense move forward in experimentally evaluating the potential of a FUV operational system.

(S) Already, the Air Force has instituted a program (Task 3) that includes the study of FUV emissions with "Chaser type" suborbital missions.

(S) We believe that the only way to provide high-angular-resolution, real-time studies of a wide variety of targets under many different observing conditions is with imaging instrumentation aboard an orbiting platform. We believe that sufficient evidence is already at hand and that favorable theoretical studies justify such a mission.

#### (U) ACKNOWLEDGMENTS

(U) We express our appreciation to Mr. R. J. Veith, who was instrumental in much of the data analysis, to Dr. P. W. Mange, the principal investigator of the OGO 4 experiment, to Dr. H. G. Wolfhard of IDA for valuable discussions during the early phases of this work, and to Mr. Larson of FTD, Wright-Patterson AFB, who assisted in the identification of some of the missile launches.

#### REFERENCES

1. T.A. Chubb, "FUV Missile Scars Observed by OGO 4," IDA Workshop on UV Plume Radiation, Arlington, Va., Feb. 1973.
2. G.R. Carruthers and T.C. Page, "Apollo 16 Far-Ultraviolet Camera/Spectrograph; Earth Observations," *J. Sci.* 177, 788-791 (1972).
3. T.A. Chubb and G.T. Hicks, "Observations of the Aurora in the Far Ultraviolet From OGO 4," *J. Geophys. Res.*, 75, 1290 (1970).
4. R.R. Meier and P. Mange, "Spatial and Temporal Variations of the Lyman-Alpha Airglow and Related Atomic Hydrogen Distributions," *Planet. Space Sci.*, 21, 309 (1973).
5. G.T. Hicks and T.A. Chubb, "Equatorial Aurora/Airglow in the Far Ultraviolet," *J. Geophys. Res.*, 75, 6233 (1970).

**SECRET**

**NRL REPORT 8061**

6. B.K. Ching, D.R. Hichman, H.R. Rugge, and J.M. Straus, "Further Considerations of Ultraviolet Missile Trails," Space and Missiles Systems Organization (SAMSO) Report TR-75-64 (Secret Report, Unclassified Title) Oct. 1974.
7. H.R. Rugge, "High Altitude UV Missile Trails," Report No. TOR-0074 (4142-01)-4, Aerospace Corp., El Segundo, Calif. (Secret Report, Unclassified Title), Aug. 15, 1973.
8. J. Myer and B. Kivel, "VUV Plume Study," Research Note 932, Avco Everett Research Laboratory, Everett, Mass. (Secret Report, Unclassified Title) Mar. 1973.
9. F.F. Marmo, "A Technical Assessment Lyman  $\alpha$  and VUV Surveillance," Report No. GCA-TR-72-15-G, GCA Corp., Bedford, Mass. (Secret), Feb. 1973.
10. W.G. Burwell, V.J. Sarli, and T.F. Zupnik, "Applicability of Sudden-Freezing Criteria in Analysis of Chemically Complex Rocket Nozzle Expansions," *Proc. AGARD Conf.* Oslo, Norway, 1966, (I. Glassman, ed.), 12, 701, AGARD, Paris, 1966.
11. J.B. Pearce, A.L. Lane, K.K. Kelly, and C.A. Barth, "Mariner 6 and Mariner 7 Ultraviolet Spectrometer: In-Flight Measurements of Simulated Jupiter Atmosphere," *Sci.* 172, 941 (1971).

**SECRET**

SECRET

## Appendix A

### FAR-ULTRAVIOLET OBSERVATIONS OF EARTH FROM THE MOON [Unclassified Title]

(S) The Hicks effect is an optical phenomenon occurring in the FUV at 1216 Å by which man-made perturbations of the near-space environment become highly visible. These perturbations of the natural scene have unique spectral and morphological characteristics that easily separate them from naturally occurring phenomena and which led to their early identification. The picture of the Earth seen in FUV wavelengths has been well documented by Carruthers' FUV photographs of Earth\* using a camera on the Moon during the Apollo 16 mission. The view obtained is strongly dependent on the spectral sensitivity of the camera and the duration of the exposure.

(U) Figure A1 shows a 5-s exposure of the Earth made by Carruthers in a spectral band of 1050 to 1600 Å. The camera employed provided a wide field of view (about 20°). The photograph shows the Earth projected against a canopy of high-temperature stars. The bright familiar, somewhat cooler stars in the visible spectrum are not observed because they are lacking in FUV emission. Figure A2 shows a 15-s exposure giving an image of the Earth. One observes the planetary image dominated by the day airglow, which reaches its highest intensity at the subsolar point. This glow is in turn dominated by emission from atomic hydrogen, which is steadily escaping from the Earth. The hydrogen glow is observed both on the day and night sides of the Earth, but it is difficult to see at night because the glow intensity is about 1/30 of that on the day side. Because of escaping hydrogen, the glow extends to very high altitude. In the longer exposure of Fig. A3 (60 s), the glow is seen extending about 60 000 km (40 000 mi) above the Earth.

(U) The hydrogen gas shown in Figs. A2 and A3 is visible because it is illuminated with FUV radiation from the Sun at the resonant transition energy of the hydrogen atom. The Earth hydrogen scatters this component of sunlight with a large cross section. This explains the visibility of the hydrogen both on the day side of the Earth and at high altitude. The Earth nightside hydrogen also glows, however. The reason this shadowed hydrogen glows is that it is also illuminated at the same wavelength by the brightly glowing high-altitude cloud of sunlit hydrogen observed in Fig. A3. Low-altitude night-side hydrogen rescatters this exospheric light.

(U) Not all the glow recorded in Figs. A1 and A2 results from the thin column of atomic hydrogen escaping from the Earth. About a third of the glow observed in the dayside of the Earth disk results from atomic oxygen. The main oxygen glow results from electron excitations, like those occurring in a neon sign. The hot electrons responsible for the glow, however, are produced by the absorption of X rays and EUV radiations contained in sunlight, instead of being the result of a voltage gradient and current flares as in the case of the neon lamp. The atmospheric oxygen glow varies in

\*G.R. Carruthers and T.L. Page, "Apollo 16 Far-Ultraviolet Camera/Spectrograph: Earth Observations," *J. Sci.* 177, 788-791 (1972).

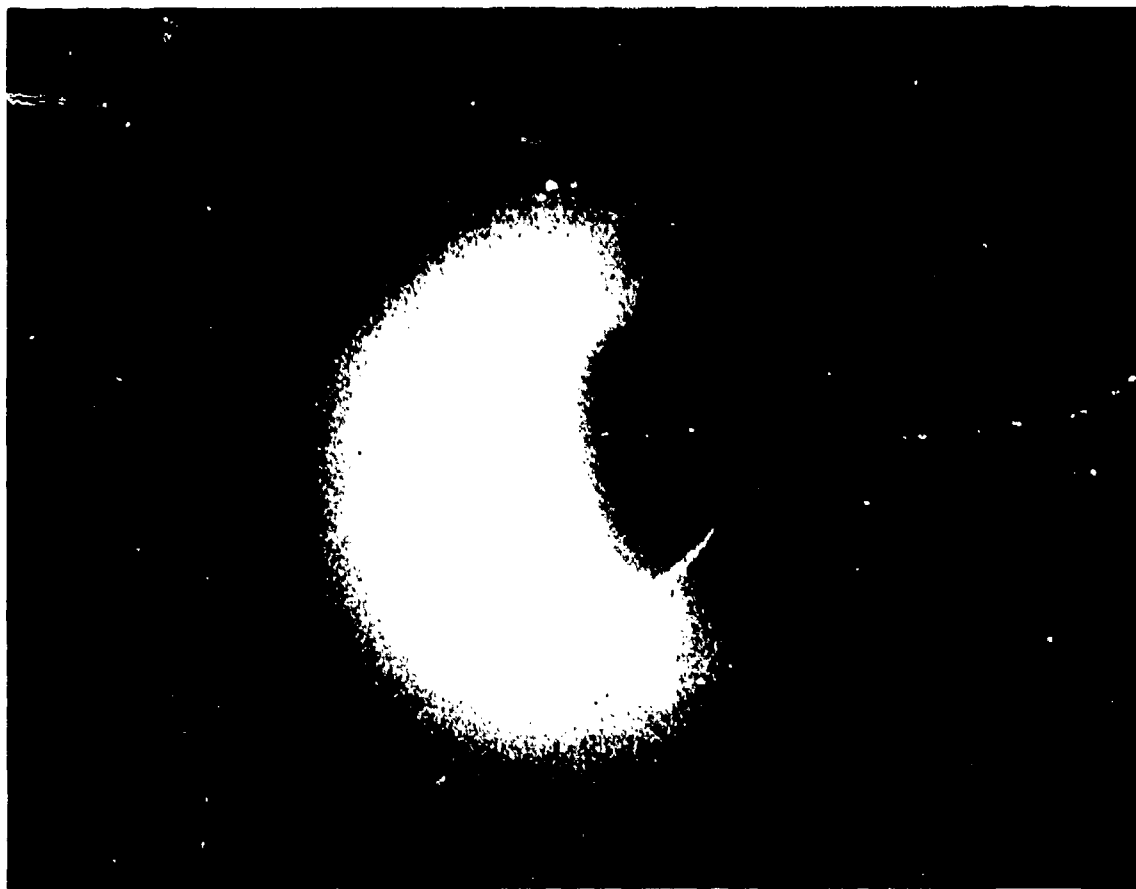


(U) Fig. A1 — Far-ultraviolet images of the Earth (wavelength range 1050 to 1600 Å) taken from the lunar surface on April 21, 1972. The exposure time was 5 s showing day airglow, polar auroras, and inner hydrogen geocorona. The northern auroral zone is discernible even on the sunlit part of the Earth.

brightness with the sunspot cycle. A third component of glow is seen in the polar regions of the Earth. This glow is a ring of light surrounding the magnetic poles. It is the polar aurora that is mainly seen in oxygen light in the FUV picture.

(U) The information provided by a space photograph of Earth is very dependent on the wavelength sensitivity of the recording camera. This fact is illustrated in Fig. A4, which is another FUV photograph of Earth made by the Carruthers camera on the Moon. In this photograph hydrogen light has been excluded from the camera so that only oxygen and nitrogen emissions are recorded. A long time exposure (10 min) was used in obtaining the photograph, so that light emission from the day glow and the aurora has caused great overexposure. The long exposure, however, reveals another little-known glow phenomenon, the equatorial FUV arcs. These arcs were discovered by Hicks and Chubb\* in the OGO 4 data. These magnetically controlled glow features are pure oxygen emissions associated with ion recombination. They are indirect results of an electric-field process

\*G.T. Hicks and T.A. Chubb, "Equatorial Aurora/Airglow in the Far Ultraviolet," *J. Geophys. Res.*, 75, 6233 (1970).

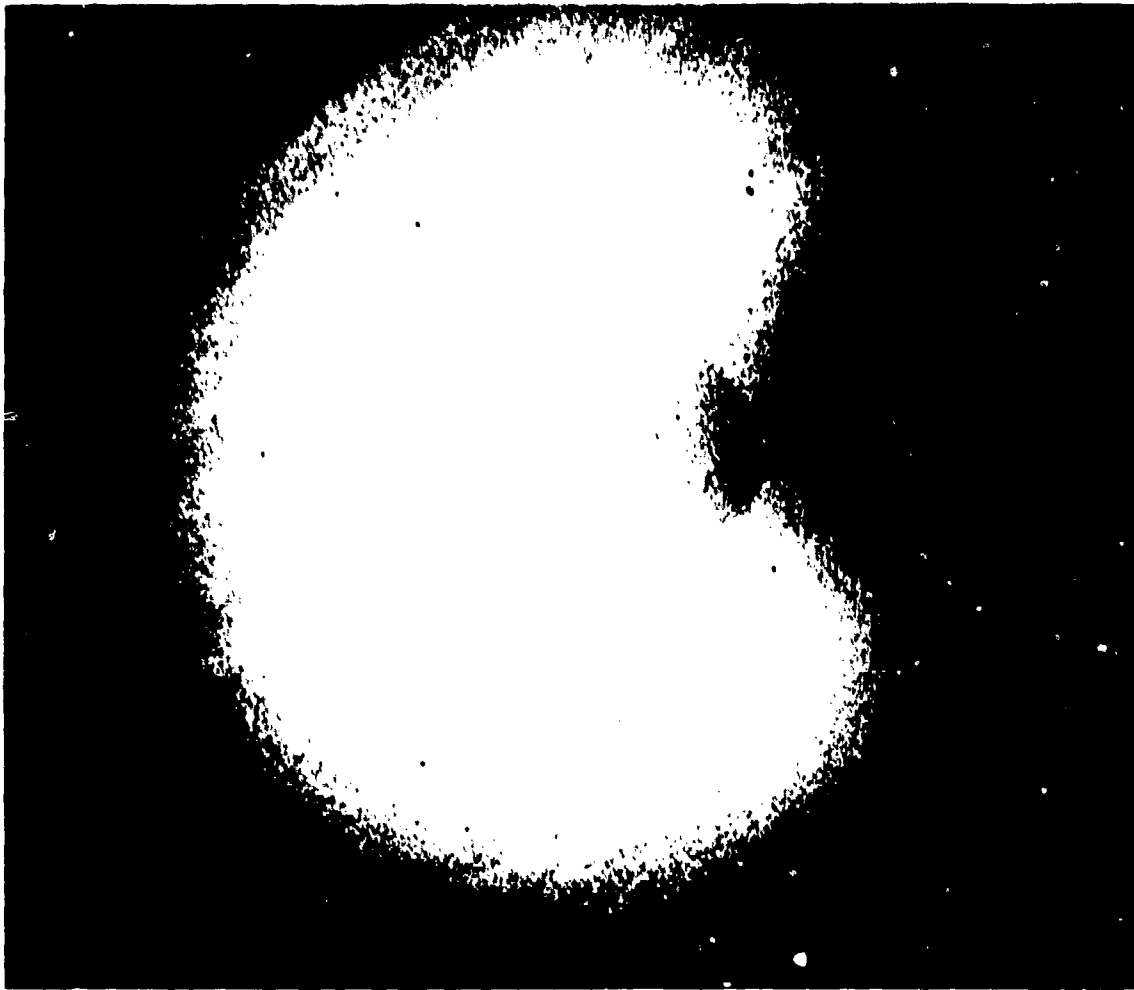


(U) Fig. A2 — A 15-s exposure (1050 to 1600 Å), showing the night-side auroral zones and the geocorona more strongly.

occurring at the magnetic-dip Equator and are closely related to the ionospheric equatorial anomaly.

(S) During the recording of the Apollo 16 photographs, no missile launchings are known to have occurred, and no information on the Hicks effect was obtained.





(U) Fig. A3 — A 1-min exposure centered on the Earth, wavelength range 1050 to 1600 Å. The hydrogen geocoronal Ly- $\alpha$  emission is the dominant feature. The dark limb is seen silhouetted against the interplanetary Ly- $\alpha$  background. The diagonal streaks in the upper portion of the picture are instrumental.

SECRET

NRI REPORT 8061



(U) Fig. A4 — Image of the Earth in the 1250- to 1600-Å wavelength range, showing dayglow, polar auroras, and tropical airglow belts. Exposure time was 10 min.

SECRET

SECRET

## Appendix B

### SUMMARY OF HICKS EFFECT EVENTS

[Secret Title]

(S) In this section we provide tabular listings of all events seen by the OGO 4 FUV radiometer. The list has been divided into two parts. The first lists those events that we associated with specific missions. These are listed in Table B1. The second group of detections, for which we were initially unable to identify missile launches, is given in Table B2. This list was transmitted to the Foreign Technology Division at Wright-Patterson AFB, which subsequently informed us that all foreign sightings could be identified with specific missions.

(S) Table B1 -- Missile Scars Attributable to Known Launches

Date	Time (UT)	Position of Maximum Signal (deg)		Associated Launch	Remarks
		Latitude	Longitude		
Apr. 4, 1968	1251.4	23.5S	72.4E	Apollo 6	Several observations made at various times and places. This observation made 6 min after Apollo 6 crossed the position listed.
Apr. 7, 1968	1238.0	49.5N	77.7E	Luna 14	—
Apr. 14, 1968	1155.2	51.3N	78.2E	Cosmos 212	—
Apr. 15, 1968	1215.3	45.1N	70.8E	Cosmos 213	—
July 5, 1968	1606.7	48.5N	63.9E	Molnyia 1J	—
July 16, 1968	1445.5	63.2N	64.4E	Cosmos 232	—
July 16, 1968	1624.0	58.9N	41.1E	Cosmos 232	—
Aug. 9, 1968	1252.4	45.9N	61.0E	Cosmos 235	—
Oct. 19, 1968	0530.3	50.0N	65.8E	Cosmos 248	—
Oct. 26, 1968	0550.4	45.2N	68.0E	Soyuz 3	—
Nov. 16, 1968	1510.0	31.7N	119.1W	KX-110	—
Jan. 14, 1969	0912.0	49.1N	69.9E	Soyuz 4	—
Jan. 15, 1969	0927.0	49.3N	64.6E	Soyuz 5	—
Dec. 21, 1968	1409.6	4.8N	26.7E	Apollo 8	Over Africa on first orbit of Apollo 8.
Dec. 21, 1968	1547.0	6.0N	2.3E	Apollo 8	Over Africa on second orbit of Apollo 8. These signals probably caused by outgassing of vehicle.
Dec. 22, 1968	0133.8	22.6N	144.0W	Apollo 8	Near Hawaii--scars left by engine firing for translunar injection that occurred 9 h 51 min and 11 h, 21 min, respectively, before these observations.
Dec. 22, 1968	0308.6	13.6N	168.2W		

(S) Table B2 — Missile Scars Initially Not Attributable to Known Launches

Date	Time (UT)	Position of Maximum Signal* (deg)		General Area†	Data Format‡	Signal Quality
		Latitude	Longitude			
Apr. 5, 1968	1332.4	51.2N	66.9E	TYUR	MC	Good
July 21, 1968	1409.5	19.4S	107.4W	—	MC	Faint but definite
July 21, 1968	1550.0	6.3S	131.7W	—	MC	Faint but definite
July 25, 1968	1527.5	17.5S	132.8W	—	MC	Faint but definite
July 28, 1968	0236.0	27.6N	124.4W	WTR	SC	Faint
Aug. 9, 1968	0106.8	47.8N	66.6E	TYUR	MC	Good
Aug. 17, 1968	0055.7	29.5N	129.2W	WTR	MC	Good <sup>  </sup>
Oct. 3, 1968	2134.2	61.2N	39.6E	PLES	MC	Good <sup>¶</sup>
Oct. 12, 1968	0640.7	51.8N	58.2E	TYUR	SC	Good

\*Position of maximum signal is the latitude and longitude between spacecraft and Earth (perigee  $\approx$  400 km; apogee  $\approx$  900 km) where signal reached a maximum value. Satellite was in a polar orbit (inclination  $86^\circ$ ); hence signal could arise from a crossing of any part of a missile trajectory having a smaller inclination angle.

†TYUR = Tyuratam; PLES = Plesetsk; WTR = Western Test Range.

‡SC refers to Subcom data, for which the data rate is slow and the data are subject to noise that can give erroneous signals if only one data point is available. At least two data points were available. MC refers to Maincom data at a rate sufficiently high to give a smoothly plotted curve.

<sup>||</sup>Possibly ESSA 7 or OV 5-8.

<sup>¶</sup>Local time was early morning, approximately 0013.

SECRET

## Appendix C

### CALCULATIONS CONCERNING DETECTION OF HIGH-ALTITUDE MISSILE BURNS (ABOVE 150 km) USING HICKS EFFECT [Secret Title]

#### CALCULATION OUTLINE

(S) This work was done in 1972 and was first presented by Chubb [C1]. This appendix is concerned with the observability by a potential surveillance system above 150 km; Appendix D discusses missile signals at 120 km; and Appendix E discusses effects between 80 and 100 km.

(S) We first calculate the background signal strength per resolution element for a potential surveillance detector and determine the integration time required for certain detection of a local 30% increase in scattering. Next we calculate the increase in local atomic-hydrogen content required to produce a 30% increase in signal over a single resolution element. Then we calculate the atomic-hydrogen content release per kilometer of trajectory required to produce the required local content. We next calculate the rocket exhaust mass flow rate required to give the needed atomic-hydrogen output in accordance with gas kinetic calculations for nozzle with a 16:1 area ratio. From this mass flow rate we calculate the engine thrust, assuming a 300-s specific impulse. The calculation applies only to high-altitude burns, because it assumes the scattering exhaust cloud to be at 1000 K. This means that the calculation should be valid at altitudes above 150 km. Finally, we extend the calculations to synchronous orbit.

#### THE CALCULATIONS

##### Signal Strength Per Resolution Element for a Potential Surveillance System

(S) The instrument is a 10-cm (4-in.) f/1.5 Schmidt camera with 8% optical and photoelectric quantum efficiency. The camera resolution is 1' of arc =  $2.91 \times 10^{-4}$  rad. The field of view is 0.23 rad ( $13^\circ$ ). Television (TV) resolution is 700 lines; TV resolution is 1.1' of arc =  $3.3 \times 10^{-4}$  rad. Overall angular resolution is 1.5' of arc =  $4.4 \times 10^{-4}$  rad.

(S) We carry out our calculations for an intermediate observation altitude of (2280 + 100) km = 2380 km (1280 n.mi.).

1. Resolution at the 100-km altitude layer = 1 by 1 km
2.  $L_y \propto$  background seen looking down from 2380 km is 40 kilorayleighs (kR) =  $3.2 \times 10^9$  photons  $\cdot$  cm $^{-2} \cdot$  s $^{-1}$  sr $^{-1}$ .
3. Solid angle subtended by resolution element  $4.4 \times 10^{-4}$  rad (1.5' of arc) by  $4.4 \times 10^{-4}$  rad (1.5' of arc) =  $1.9 \times 10^{-7}$  sr.

4. Area of sensor (assuming 70% nonocculted opening) is  $57 \text{ cm}^2$ .
5. Combined optical and photoelectron efficiency is 0.08.
6. Each resolution element on photocathode will deliver  $3.2 \times 10^9 \times 57 \times 1.9 \times 10^{-7} \times 0.08 = 2.77 \times 10^3$  photoelectrons per second.

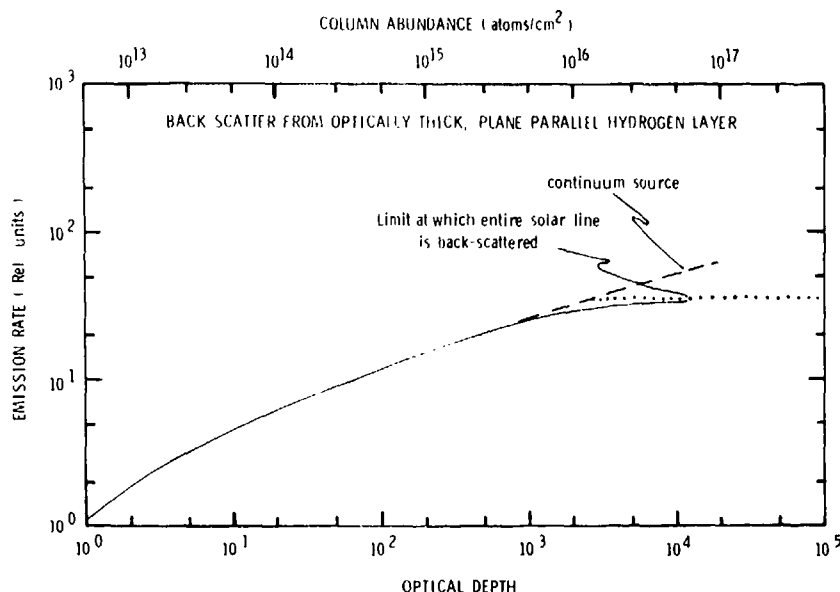
(S) We use as our requirement for certain detection that the increase in signal from a resolution element exceed the statistical fluctuations in background by 7. For an increase in signal by a factor of 1.3, this condition is met when 544 electrons have been ejected from the photocathode. The integration time required to record a for-sure detection from a local region in which a 30% increase in signal occurs is  $544/(2.77 \times 10^3) = 0.2 \text{ s.}$

#### (S) Observability of a Missile Trail Above 150 km

(S) In this section we compute the increase in local atomic-hydrogen content required to locally increase the upward Ly  $\alpha$  flux by 30% during the day. Other more elaborate computations including photochemistry are given in the references [C2-C5].

(S) The natural Lyman  $\alpha$  background results from scattering of sunlight by atmospheric hydrogen atoms produced by dissociation of  $\text{H}_2\text{O}$ ,  $\text{H}_2$ , or methane in the 80- to 100-km level of the atmosphere. The dissociation products continuously escape from the Earth because Earth's gravity is too low to hold a particle of 1 proton mass at thermospheric temperature. The spatial-altitude distribution of naturally occurring atomic hydrogen has been determined by model fitting, in which the intensity of Lyman  $\alpha$  as observed from rockets and satellites, as a function of solar-zenith angle, altitude, and direction of view, is matched to computed intensities based on the assumption that the glow is produced by multiply scattered solar photons. The calculations do a good job in explaining the glow observations, and leave no doubt regarding the origin of the Lyman  $\alpha$  geocoronal glow [C6]. They also lead to models of the atomic-hydrogen distribution in Earth's outer atmosphere. These models show that the vertical equivalent Lyman  $\alpha$  optical depth at 150 km altitude is 1.87 and that the corresponding naturally occurring overhead column density is  $1.3 \times 10^{13} \text{ cm}^{-2}$  of hydrogen atoms. This hydrogen is at a temperature varying from 750 to 1100 K. Below 150 km the temperature drops with increasing rapidity to about 200 K at 100 km. The column density of atoms above 100 km is estimated to be  $10^{13} \text{ cm}^{-2}$ .

(S) The Hicks effect is the result of increased scattering of the solar 1216-Å line resulting from local increases in atomic-hydrogen content. To locally increase the scattering of sunlight by 30% requires an increase in the local optical depth from 6 to 10.2. Figure C1 shows a theoretical curve for backscattered Ly  $\alpha$  as a function of column depth. The column depth is in units of line center optical depth, which for 1000-K hydrogen is in units of  $5.27 \times 10^{12} \text{ atoms cm}^{-2}$ . The intensity is in units of 16 kR. The total hydrogen column has roughly the same appearance from above as a column of 1000-K hydrogen with an optical depth of 6. The required increase in column density is  $2.3 \times 10^{13} \text{ cm}^{-2}$  of hydrogen atoms. This calculation applies only for hydrogen at 1000 K. Hence, the calculation applies to a hydrogen cloud located at an altitude above 150 km.



(U) Fig. C1 — Theoretical curve of growth of backscattered Lyman  $\alpha$  airglow as a function of H column optical depth. The curve of growth assumes a finite-thickness, horizontal slab of atomic hydrogen at a constant temperature  $T$ . The slab is illuminated from above with a source of collimated, Ly- $\alpha$  photons directed vertically downward onto the slab. The incident Ly- $\alpha$  photons are assumed to be derived from a broad line with a constant intensity per angstrom near the line center. The abscissa is the line-center vertical optical depth at the bottom of the slab. The ordinate is in units of relative intensity. The value of a unit of intensity depends on the temperature of the slab and the line center intensity of the source. For 350-K hydrogen and a nominal solar photon flux input of  $5 \times 10^{11} \text{ cm}^{-2} \text{ s}^{-1} \text{ \AA}^{-1}$ , a unit of relative intensity equals 7.48 kR. For 1000-K hydrogen a unit of relative intensity equals 12.6 kR. At  $\tau = 1$ , the column density is  $5.37 \times 10^{12} \text{ cm}^{-2}$  column at 1000 K.

(S) We are concerned with cloud detection at the time when the exhaust trail from a missile is 1 km in diameter. For definiteness we imagine a trajectory at an elevation angle of  $45^\circ$ . For a  $45^\circ$  inclined column the vertical depth through the cylindrical column is  $\sqrt{2}$  times the column diameter. However, we will ignore this favorable factor, because we will treat the trail as if it were rectangular, and we will use a length of side equal to the diameter. Thus far in this simplified approximation we assume that we require an increase of  $2.3 \times 10^{13} \text{ cm}^{-2}$  of hydrogen atoms over a  $1\text{-km}^2$  area for each kilometer of vehicle trajectory. Thus, the required atomic-hydrogen release rate is  $2.3 \times 10^{13} \times 10^{10} = 2.3 \times 10^{23}$  hydrogen atoms per kilometer of vehicle trajectory. Now, at a velocity of 6.45 km/s (4 mi/s) the release rate required is  $2.3 \times 10^{23} \times 6.45 = 14.5 \times 10^{23} \text{ s}^{-1}$  of atoms.

(S) The conclusion is that any rocket at an approximately  $45^\circ$  trajectory releasing  $14.5 \times 10^{23} \text{ s}^{-1}$  of hydrogen atoms will produce an expanding exhaust trail that will locally increase the scattering of solar Lyman  $\alpha$  photons by 30% when it reaches a diameter of 1 km. (It will be even brighter when smaller.)

(S) Mass Flow Rate From Rocket Exhaust  
Required To Increase Signal by 30%

(S) We have shown that an atomic-hydrogen release rate of  $14.5 \times 10^{23}$  atoms  $s^{-1}$  at an altitude above 150 km will produce a trail, which when it becomes 1 km wide, will increase the natural Ly  $\alpha$  background by 30%. We now ask, what total rocket exhaust flow rate must be expelled to produce this required flow rate of atomic hydrogen? This calculation requires a knowledge of the atomic-hydrogen concentration in the rocket exhaust. Moreover, the exhaust calculation must be realistically done for the following reasons:

1. In the combustion chamber itself, temperatures are high enough to produce high concentrations of atomic hydrogen. If one assumes that these concentrations prevail in the exhaust, one gets an unrealistically optimistic view of the amount of exhausted atomic hydrogen.

2. On the other hand, if one assumes that full thermal equilibrium prevails at all points along the nozzle and calculates equilibrium values for the atomic hydrogen that prevails at the exit plane of a highly expanded nozzle, one calculates an unrealistically low value of atomic hydrogen concentration in the exhaust.

3. The only meaningful exhaust composition calculation for this problem is a lagging equilibrium calculation in which full attention is paid to the minor constituents.

Calculations in which all known kinetic reactions are included have been carried out by Burwell, Sarli, and Zupnik [C7]. In these calculations the gas conditions are determined by reaction rates point by point down through the nozzle throat and down the exhaust cone. They show that atomic hydrogen is quickly "frozen out" and does *not* follow a shifting equilibrium concentration calculation. The authors calculate for a 410-k Pa (60-psi) engine, running on  $N_2O_4$ -Aerozine fuel, a H/ $H_2O$  mole ratio of 0.095 at an area ratio of 16, with the H/ $H_2O$  ratio almost independent of area ratio. This H/ $H_2O$  ratio compares with a value of 0.0195 reported in the *Handbook of Military Infrared Technology* [C8] for an engine using inhibited red fuming nitric acid (IRFNA) and unsymmetrical dimethylhydrazine (UDMH). Unfortunately, Burwell, Sarli, and Zupnik do not give the full composition of the exhaust products. We therefore use the values from the *Handbook of Military Infrared Technology* for everything except H, which we take as 10% of the  $H_2O$ . The values used are shown in Table C1, with the handbook value for H shown in parentheses.

(S) The required atomic-hydrogen exhaust rate is  $14.5 \times 10^{23} s^{-1}$ , which corresponds to an atomic-hydrogen mass flow rate of  $14.5 \times 10^{23} \times 1.67 \times 10^{-24} = 2.42$  g/s. The total engine exhaust flow delivering this atomic hydrogen content is  $2.42/0.00174 = 1.39$  kg/s, (3.07 lb/s), of fuel and oxidizer. If the specific impulse of the engine is 300 s, we can expect the prompt detectability of a 418-kg (920-lb) engine.

Detection of Submarine-Launched Ballistic Missiles Using  
Daylight Hicks Effect From Synchronous Orbit

(S) We envision a set of f/6.6 FUV telescopic image converters, 31 cm (12 in.) in aperture, giving a field of view of 1 by 1 Mm at Earth with a resolution of 1 by 1 km, as readout by a 1000-line-resolution TV system. The working distance is about 25 000



(S) Table C1 — Composition of Exhaust Products

Molecule	Mole Percent	Mole Weight	Weight Fraction
H <sub>2</sub> O	35.3	18	0.317
H <sub>2</sub>	19.1	2	0.019
H*	3.5 (0.69)	1	0.00174 (0.000344)
OH	0.24	17	$1.7 \times 10^{-3}$
O	0.1	16	$8.0 \times 10^{-4}$
NO	0.02	30	$3.0 \times 10^{-4}$
N <sub>2</sub>	22	28	0.307
CO <sub>2</sub>	4.74	44	0.104
CO	17.5	28	0.244
HF	0.53	20	0.005

\*Values in parentheses are from the *Handbook of Military Infrared Technology* [C8].

mi = 40 Mm. The TV sensor target is envisioned as a 25-by-25-mm element (thereby having a 35-mm diagonal), so that size of a resolution element is 0.025 by 0.025 mm, and the required telescope focal length is 1 m.

1. Background Ly  $\alpha$  seen from synchronous altitude:  $44 \text{ kR} = 3.5 \times 10^9 \text{ photons. cm}^{-2} \text{ s}^{-1} \cdot \text{sr}^{-1}$ .
2. Solid angle subtended by 1 by 1 km is  $6.25 \times 10^{-10} \text{ sr}$ .
3. Area of sensor (assuming 70% nonocculted opening) is  $511 \text{ cm}^2$ .
4. Optical and photoelectron efficiency is 0.08.
5. Each resolution element on the photocathode will deliver photoelectrons at a rate of  $3.5 \times 10^9 \times 511 \times 6.25 \times 10^{-10} \times 0.08 = 89.4 \text{ el s}^{-1} \text{ per pixel}$ .

(S) Contrast criterion chosen for detection at synchronous orbit is 20%. This means that a pixel containing the source produces 17.9 electrons per pixel per second above a background of 89.4 electrons per pixel per second thus a  $3\sigma$  detection for a single pixel requires 2.5 sec.

(S) The remainder of the synchronous-orbit-detection calculation is identical with that discussed before.

(S) It is concluded that Hicks effect detection of SLBM with the use of 31-cm (12 in.) optical systems at synchronous orbit can be assured within 2.5 s of the time a 418-kg (920 lb) engine fires at 150 km or above.

## REFERENCES

- C1. T.A. Chubb, "FUV Missile Scars Observed by OGO-4," IDA Workshop on UV Plume Radiation, Arlington, Va., Feb. 1973.
- C2. B.K. Ching, D.R. Hichman, H.R. Rugge, and J.M. Straus, "Further Considerations of Ultraviolet Missile Trails," SAMSO Report TR-75-64 (Secret Report, Unclassified Title), Oct. 1974.
- C3. H.R. Rugge, "High Altitude UV Missile Trails," Report No. TOR-0074 (4142-01)-4, Aerospace Corp., El Segundo, Calif. (Secret Report, Unclassified Title), Aug. 15, 1973.
- C4. J. Myer and B. Kivel, "VUV Plume Study," Research Note 932, Avco Everett Research Laboratory, Everett, Mass. (Secret Report, Unclassified Title), Mar. 1973.
- C5. F.F. Marmo, Report No. GCA-TR-15-G, GCA Corp., Bedford, Mass. (Secret, Feb. 1973).
- C6. R.R. Meier and P. Mange, "Spatial and Temporal Variations of the Lyman-Alpha Airglow and Related Atomic Hydrogen Distributions," *Planet. Space Sci.*, **21**, 309 (1973).
- C7. W.G. Burwell, V.J. Sarli, and T.F. Zupnik, "Applicability of Sudden-Freezing Criteria in Analysis of Chemically Complex Rocket Nozzle Expansions," *Proc. AGARD Conf. Oslo, Norway, 1966* (I. Glassman, ed.), **12**, 701 AGARD, Oslo.
- C8. *Handbook of Military Infrared Technology*, W.L. Wolfe, ed., Office of Naval Research, Washington, D.C. 1965.

SECRET

#### Appendix D

#### OBSERVABILITY OF HICKS EFFECT AT 120 km

[Secret Title]

(S) In this section, we estimate the observability of a missile trail at 120 km. This condition must be considered separately from the 150-km situation, because the illuminating radiation must first pass through the atmospheric hydrogen above 150 km.

(S) A schematic diagram of the model atmosphere is shown in Table D1.

(S) Illumination of hydrogen below 150 km by both Sun and by glowing hydrogen above 150 km is assumed to be 47% of incident solar flux. This value is the ratio of the number of scattered photons passing through a slab of optical depth 2 to the total number of photons scattered within the slab and hence is a lower limit to the line center illumination applied to the 100- to 150-kR hydrogen.

#### CALCULATION PROCEDURE

1. The glow that would be produced by the  $2.41 \times 10^{13}$  atoms  $\text{cm}^{-2}$  between 100 and 150 km if these atoms were illuminated by raw vertical sunlight, assuming that all atoms are at an atmospheric temperature of 350 K, is computed from curve of growth.

(U) Table D1 — Model Atmosphere

Height (km)	Column Density of Atoms ( $\times 10^{13} \text{ cm}^{-2}$ )	Total Optical Depth	Temperature (K)	Comments
>150	—	—	1000	Hydrogen above 150 km is treated as a slab at 1000 K. Photons attenuated at $e^{-1.87}$ .*
150	1.31	1.87	~760 ~350 ~200	Hydrogen between 100 and 150 km is treated as if it were all at 350 K.*
120	1.58	2.33		
100	3.72	17.5		
<100	—	—	—	Hydrogen below 100 km is estimated to be twice that above 100 km, but its contribution is neglected because of its 200-K temperature.

\*Attenuation of exciting incremental flux is assumed the same as at line center, for hydrogen above 150 km, but no attenuation is assumed between 120 to 150 km, because incremental photons are outside core of 350-K column.

2. The glow that would be produced by a slab of density  $12.41 \times 10^{13} \text{ cm}^{-2}$  (the mentioned  $2.41 \times 10^{13} \text{ cm}^{-2}$  with an additional exhaust column of  $1.0 \times 10^{14} \text{ cm}^{-2}$ ) is computed.

3. The difference in the glows mentioned is the scar contribution.

4. The scar contribution is multiplied by 0.47 to take into account the reduction in incident flux by the hydrogen above 150 km and is reduced by  $\exp(-1.87)$  to take into account the loss in local source brightness because of the column scattering at line center above 150 km.

### (S) CALCULATIONS

(S) At 350 K the line center scattering cross section is  $3.13 \times 10^{-13} \text{ cm}^2$ . For no exhaust the line center optical depth at 100 km is

$$2.41 \times 10^{13} \times 3.13 \times 10^{-13} = 7.54.$$

For 350-K hydrogen a relative emission rate of 1 on the curve of growth corresponds to 9.47 kR. With the curve of growth, an optical depth of 7.54 then gives a backscatter intensity  $I_B$  of

$$I_B = 4.0 \times 9.47 = 38 \text{ kR}$$

when illuminated by raw sunlight.

(S) When the column density is increased by  $1.0 \times 10^{14} \text{ cm}^{-2}$  to a total of  $1.24 \times 10^{14} \text{ cm}^{-2}$ ,

$$\tau = 38.8,$$

and, again, with the curve of growth the total intensity  $I_T$  is

$$I_T = 8.2 \times 9.47 = 77.7 \text{ kR}$$

The net scar intensity  $I_S$  is, then,

$$I_S = 77.7 - 38 \approx 40 \text{ kR}.$$

Observed scar intensity  $I_{SO}$  after attenuation by overhead hydrogen above 150 km and with 47% illumination is

$$I_{SO} = 40 \times 0.47 \times 0.154 = 2.90 \text{ kR}.$$

(S) Total observed background (backscattered) flux  $I_{BO}$ , including scattering from the hydrogen above 150 km, as observed from 2380 km, is

$$I_{BO} = 40 \text{ kR}.$$

Signal contrast is 7.2%.

SECRET

## Appendix E

### DETECTION OF MISSILES BY LINE-WING RADIATION

[Secret Title]

(S) The analyses conducted so far have been based on the assumption that the upward net velocity of the rocket exhaust will propel the exhaust upward at a rate of about 1.2 km/s until the exhaust extends above about 120 km, at which altitude the curve-of-growth method of computing intensification of the Ly  $\alpha$  glow is reasonably accurate. It is believed that exhaust escape may occur from as low as 80 km. This upward flow, however, takes a moderate period of time. In this section we explore the detectability of the hydrogen while it is still in the 90- to 100-km level. We assume that the hydrogen is essentially at an ambient temperature of 200 K. We assume that diffusive separation of H is not effective, so that the natural relative H concentration remains constant between 100 and 115 km, which probably leads to an overestimate of hydrogen below 115 km.

(S) The isothermal curve-of-growth method of calculating backscattered Ly  $\alpha$  is inappropriate below 100 km, because the high column depth of warm atomic hydrogen overhead removes the core from the solar Ly  $\alpha$  line. As a result the narrow doppler width of even substantial thicknesses of 200-K hydrogen means that little is added to the scattering near the core. There is, however, a component of scattering in the line wings that is subject to exact calculation and that does not involve the complication of complete frequency redistribution, which would lead to radiation entrapment if it occurred. In this section we calculate the line-wing component of scattering, which will be visible to below 90 km.

(S) Meier and Prinz have carried out calculations of the equivalent width and profile of the absorption core in the solar Ly  $\alpha$  line as viewed from varying altitude. These calculations include the temperature variation of the real atmosphere. At 95 km the optical depth at line center is 17.5 and the equivalent width of the absorption core is 0.040 Å. In units  $x$  of the doppler width  $\Delta\lambda_D$  of hydrogen at 200 K ( $\Delta\lambda_D = 0.00744$  Å), the overhead optical depth = 0.1 at  $|x| = 4$ . Thus, all the Ly  $\alpha$  line for which  $|x| > 4$  has a clear view of space and is subject only to O<sub>2</sub> absorption, for which  $\tau = 1/2$  at 82 km. We therefore ask the amount of Ly  $\alpha$  scattering to be expected from the line wings.

(S) The incremental equivalent width  $\Delta W$  from wing scattering in the solar line because of passage through a layer of 200-K hydrogen of optical depth  $\tau$  is given by

$$\Delta W = 2 \int_4^{\infty} (1 - e^{-\tau}) dx,$$

where  $x = \lambda - \lambda_0$  is in units of  $\Delta\lambda_D$ . For  $x > 2$ ,

$$\tau = \tau_0 \frac{a}{\sqrt{\pi}} \frac{1}{x^2}.$$

For hydrogen at 200 K,  $a = 0.0033$ ,  $\Delta\lambda_D = 0.00744$ , and

$$\Delta W = \Delta\lambda_D \tau_0 \frac{0.0033}{\sqrt{\pi}} \left( \frac{1}{4} \right) = 3.46 \times 10^{-6} \tau_0.$$

The broad solar line contains a photon flux  $\mathcal{F}$  of  $5 \times 10^{11} \text{ cm}^{-2} \text{ s}^{-1} \text{ \AA}^{-1}$ . The line center scattering cross section  $\sigma_0$  for 200-K hydrogen is  $4.12 \times 10^{-13} \text{ cm}^2$ . The scattered flux for a column of hydrogen  $N$  is then given by

$$\begin{aligned} F_s &= \Delta W \mathcal{F} \sigma_0 N \\ &= 3.46 \times 10^{-6} \times 5 \times 10^{11} \times 4.12 \times 10^{-13} N \\ &= 7.13 \times 10^{-7} N. \end{aligned}$$

Now an airglow layer that emits in all directions a photon flux of  $10^9 \text{ cm}^{-2}$  column is said to emit 1 kR of radiation. Thus, in terms of kilorayleighs,

$$F_s = 0.713 N_{15}$$

where  $N_{15}$  is the hydrogen column depth in units of  $10^{15} \text{ cm}^{-2}$ .

(S) Let us return to the consideration of a 34 000-kg (75 000-lb) rocket expelling gases in accord with the calculations of Burwell, Sarli, and Zupnik.\* At the time the exhaust trail has expanded to 1 km in diameter, the column depth  $N$  will be  $1.74 \times 10^{15} \text{ cm}^{-2}$  of atoms and the backscattered wing Lyman  $\alpha$  will be 1.24 kilorayleighs. (Note that for this optically thin case the total scattered flux is independent of column diameter.) The trail will be visible at a contrast ratio of 3.1%. To observe a signal of 3.1% contrast with  $7\sigma$  requires 51 000 photoelectrons per resolution element. At the 40 kR background glow assumed in determining the contrast, a low-altitude surveillance detector will require an integration period of 1.8 s. For the wing-scattered signal there is little effect due to solar zenith angle and viewing zenith angle. As a result, this calculation also applies to a worst case  $70^\circ$  solar zenith angle and a  $70^\circ$  solar viewing angle. At synchronous orbit the contrast is reduced to 2.5%. A 61-cm (24-in.) optical system with 1 km of resolution will provide  $7\sigma$  signals in 22 s.

(S) It should be noted that a synchronous orbit detection system working on line-wing radiation would probably best be designed using an internal atomic-hydrogen scattering cell to suppress the ambient line-center radiation, which makes up most of the back-scattered background. Such a system would greatly increase the wing signal contrast. Such cells have been flown in rockets and satellites. They would not be suitable for a small-f-number optical system.

\*(U) W.G. Burwell, V.J. Sarli, and T.F. Zupnik, "Applicability of Sudden-Freezing Criteria in Analysis of Chemically Complex Rocket Nozzle Expansions," *AGARD Conf. Proc.* (I. Glassman, ed.), 12, 701, Oslo, Norway, 1966.



DEPARTMENT OF THE NAVY  
NAVAL RESEARCH LABORATORY  
4555 OVERLOOK AVE SW  
WASHINGTON DC 20375-5320

IN REPLY REFER TO:

5510  
Ser 1221.1/0005  
2 Feb 98

From: Commanding Officer, Naval Research Laboratory  
To: Chief of Naval Research (Code 93)  
Subj: REQUEST DISTRIBUTION STATEMENT CHANGE  
Ref: (a) NRL memo Ser 7640/006 of 9 Jan 98  
Encl: (1) NRL Report 8061, "Far Ultraviolet Studies of Missile Trails"

1. Per reference (a), request the distribution statement of enclosure (1) be changed to unlimited.
2. If more information is required, please contact me at (202) 767-2240 or Dr. Robert R. Meier at (202) 767-2773.

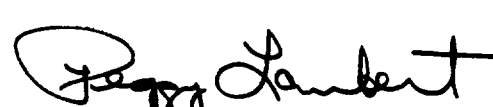
  
CHARLES ROGERS  
By direction

---

5510/6  
Ser 93/205  
17 Feb 98

From: Chief of Naval Research  
To: Commanding Officer, Naval Research Laboratory  
Subj: CHANGE OF DISTRIBUTION STATEMENT

1. Permission is granted to change distribution statement to A: Unlimited Distribution.
2. Please notify Mr. Bill Bush, DTIC-OCQ, (703) 767-0011, of the change.
3. Questions may be directed to the undersigned on (703) 696-4619.

  
PEGGY LAMBERT  
By direction

*Completed*  
*15 May 2000*  
*B.W.*

AD-C008 887